COMPUTERS AND BIOMEDICAL RESEARCH 7, 380–394 (1974)

A Technique for the Detection of Asynergistic Motion in the Left Ventricle*

LOWELL D. HARRIS, PAUL D. CLAYTON, HIRAM W. MARSHALL, AND HOMER R. WARNER

Latter-day Saints Hospital, Cardiovascular Laboratory, Salt Lake City, Utah 84143

and

Department of Biophysics and Bioengineering, University of Utah, Salt Lake City, Utah 84143

Received November 7, 1973

A method is described whereby 60/second, monoplane, video images of the opacified left ventricle are digitized and the location of the endocardial surface is determined by a computer-based algorithm. For each contour, representing the location of the endocardial surface in a single plane at a given point in time, a reference point is defined as the midpoint of a straight line connecting the center of the aortic valve to the apex. The radial distances from the reference point to the contour are determined at five-degree increments around the contour for each of the contours during systole. The correlation coefficients and linear regression slopes for each radius sequence versus the mean radius sequence are calculated and plotted. The correlation coefficient and linear regression slope means and ranges are determined for normal hearts and then compared with the values from a heart demonstrating an abnormal pattern. By a computer method, the location and characteristics of the motion abnormality are described.

INTRODUCTION

The acceptance of the concept that myocardial performance can best be described in terms of myocardial mechanics (*1*) and evidence that the presence of motion disorders (asynergy) of the left ventricular wall reduces the efficiency of left ventricular contraction and thereby can contribute to the development of heart failure (*2, 3*) have led to the development of techniques for acquiring dynamic dimensional data from the left ventricle and for locating segments of the ventricular wall demonstrating abnormal motion patterns. Some of the current methods used to gather information about left ventricular dynamic geometry include: radiopaque markers attached to the myocardium (*4–8*), dimension gauges (*9–14*), echocardiography (*15*), radarkmography (*16*), and cine and videoangiocardiography (*17–20*). In addition, the

* Supported by Grant No. HF04664 held conjointly with Mayo Clinic, Rochester, Minn., and USPH Grant No. RR-00012, University of Utah, Salt Lake City, Utah.

method of apex or kinetocardiography (*21*) has been used to locate segments of the myocardium which demonstrate asynergistic motion even though the method does not yield direct dimensional information. The purpose of this report is to describe a mathematical model of the motion of the canine left ventricle during systole from single plane videoangiocardiographic data which not only yields a description of the dynamic geometry of the left ventricle but also provides a method whereby wall motion disorders can be located and quantitated.

Methods

Biological Preparation

The dogs used in this study were preanesthetized with morphine sulphate (1.5 mg/kg body weight) and then anesthetized with sodium pentobarbitol after a delay of 45 minutes. Three catheters were inserted into the circulation to monitor the left ventricular and aortic pressures and to inject the radiopaque contrast media. After catheterization, the animal was placed in a half-body cast and suspended in the X-ray field in a right anterior oblique (RAO) projection. The dogs were maintained on intermittent positive-pressure ventilation which was suspended during the injection of the contrast media to obviate the effects of respiration on heart position and motion. In three preparations there was a variation in the procedure to produce ventricles with abnormal contraction patterns. After recording several injections of contrast media into the normal ventricle, the dye injection catheter was removed and a Sones No. 7 catheter was inserted and positioned in the anterior descending branch of the left coronary artery. After verifying catheter position by the injection of a small amount of contrast media, 0.1–0.2 ml of mercury were injected in order to occlude the blood supply to a portion of the ventricular wall. This method, described by Lluch as a technique for generating cardiogenic shock (*22*), was used to damage a portion of the myocardium and thereby produce wall motion disorders.

Video Data Generation

The video angiocardiographic data used in this study is generated in the conventional manner by injecting a radiopaque contrast agent into the left ventricle and then recording the video representation of the event on a video disc recorder (Ampex DR10A) under computer control. The injection of the dye is controlled using the computer to avoid the useless loss of contrast agent which would occur if it were injected too early in the heart cycle. The video disc is computer controlled so that the time relationship between the video and concomitant physiological data can be preserved.

Image Processing

The first step in processing the video data is to determine which video frames are to be processed by the computer program to represent one complete systole. The

program reviews the left ventricular and aortic pressure data and locates end diastole (LVED) from the left ventricular pressure and end systole (dicrotic notch) from the sampled aortic pressure data. It then determines which video fields correspond to these two points in the heart cycle and displays the frame numbers back on the computer terminal. The video disc is then positioned at the video frame corresponding to end diastole and left in the stop action mode. The next step in the processing of the video data is to determine the internal border (contour) of the left ventricle for each video field during systole. This process is carried out by the contour determination program developed over the past several years at this facility. The process involves digitizing the stop action single frame video picture of the opacified ventricle and then finding the left ventricular border using a probabilistic border search algorithm described elsewhere (*23*). In this manner a sequence of contours is determined which represents the position of the left ventricular endocardial surface during systole in a given plane. The contour determination program operates from a remote terminal which allows the investigator to constantly review the output of the computer border algorithm superimposed on the original X-ray image. Manual changes may be made if the operator disagrees with the computer determined border on any frame. Once a contour sequence is determined, reviewed and accepted, the data are stored on magnetic digital disc for further analysis. In addition to the border points, the contour determination program also finds the apex point and the right and left sides of the aortic valve.

THE MODEL

The Calculation of Correlation Coefficient and Linear Regression Slope

The model of left ventricular wall motion during systole is generated from the contour sequence just described. The first step in this process is to determine, for each contour, the radial distances from a reference point within the contour to the contour itself at 5 degree increments as shown in Fig. 1. The reference point is defined as the midpoint of the line connecting the apex and the center of the aortic valve. This step yields 72 measures of how far the heart wall is from the reference point at a given point in time. This process is carried out for each of the contours in the sequence during systole. The radius data can then be looked upon as 72 sequences of time (r_t) representing the heart wall distance from the reference point at every five degrees. In addition, the 72 radii for each field can be summed and divided by 72 to yield the average radius sequence ($\bar{r}$), which also is a function of time.

The next step is to calculate the correlation coefficient and linear regression slope for each r_t vs $\bar{r}$ and then plot these two statistics for each angle as shown in Fig. 2. For orientation purposes it should be noted that the reference point and coordinate system are set up so that the zero degree angle is at the center of the aortic valve and the apex is therefore by definition at 180°. The mitral valve subtends an arc of about 35° at an angle near 45°. The region from about 80° to 160° is the septal

and posterior free wall. The rest of the angles from 200° to 345° are the radial measurements to the free anterior wall of the left ventricle in the right anterior oblique (RAO) position.

An illustration using an extreme hypothetical model of the left ventricle might help in understanding Fig. 2. If the ventricle were a uniformly contracting sphere, the contour sequence representing wall position during systole would be a set of

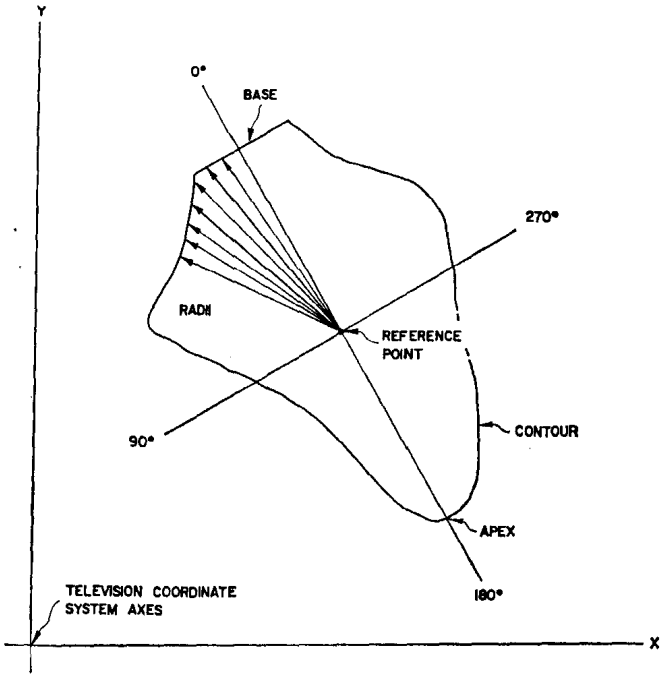

FIG. 1. A diagram showing the reference system used to determine the 72 radii from the computer determined contour. The reference system is a right-handed rectangular coordinate system with its origin at the midpoint of the line connecting the apex to the center of the aortic valve. Zero degrees is at the aortic valve and the apex is therefore at 180°. The radii are measured at 5 degree increments around the contour.

uniformly contracting circles and all the radial sequences r_i, and the average radius sequence $\bar{r}$, would be identical. The correlation coefficients and linear regression slopes for each r_i vs $\bar{r}$ would equal +1. By comparison, the plot of regression slopes for an actual contraction shows some segments of the ventricular wall, with regression slopes greater than +1, move toward the reference point more rapidly than the average radius while other segments, with regression slopes less than +1 move more slowly. In other terms, those portions of the cardiac wall contracting most vigorously and moving most rapidly towards the reference points will have the greatest regression slopes, while the regression slopes will be less for hypokinetic and akinetic segments of the ventricular wall and negative for segments with paradoxical motion.

The difference between the plot of the correlation coefficients in Fig. 2 and the corresponding plot for the hypothetical example of a uniformly contracting sphere arises from two causes. First, there is the random error in the computer determined border position which induces scatter in the plots of r_i vs $\bar{r}$ and thereby lowers the correlation coefficient below +1. It is this random error, due in part to "noise" in

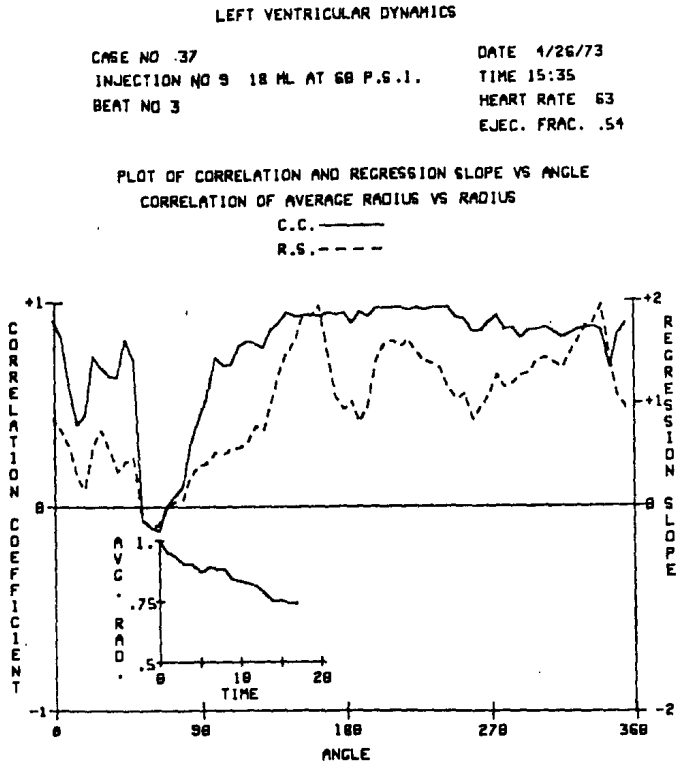

FIG. 2. A computer generated plot of correlation coefficients (solid line) and linear regression slopes (dashed line) as a function of angle. The lower plot shows normalized average radius as a function of time in units of 1/60th of a second or number of fields. Values of correlation and linear regression slope at 180° describe the motion of the apex. The aortic systolic valve motion is described by the values above 345° and below 15° while the mitral valve motion is reflected in the values of the plots about 15° on either side of the 50° radius. The beat described here showed normal electrical conduction through the ventricles and was preceded by an electrically normal beat.

the X-ray signal, which causes the correlation coefficient to drop to near zero for akinetic wall segments because it is the only motion observed for such segments. The second factor causing lowered correlation coefficients arises when any of the radial sequences r_i, do not bear a linear relationship with the mean radius sequence $\bar{r}$. Plots of data generated in this study indicate that the assumption of linearity is a reasonable approximation for the normal heart, since correlation is high (.90 to .99) for most of the ventricular wall during postextrasystolic contractions (see Fig. 4).

Correlation Coefficient and Linear Regression Slope Plots for Varying Physiological and Pathological Conditions

Figures 2, 3, and 4 are representative plots of the correlation coefficients and linear regression slopes for three physiologically different left ventricular contractions. The data in the first two figures are from normal contractions but with different heart rates and ejection fractions while the data in Fig. 4 is from a post-extrasystolic contraction. All three beats had normal electrical conduction patterns

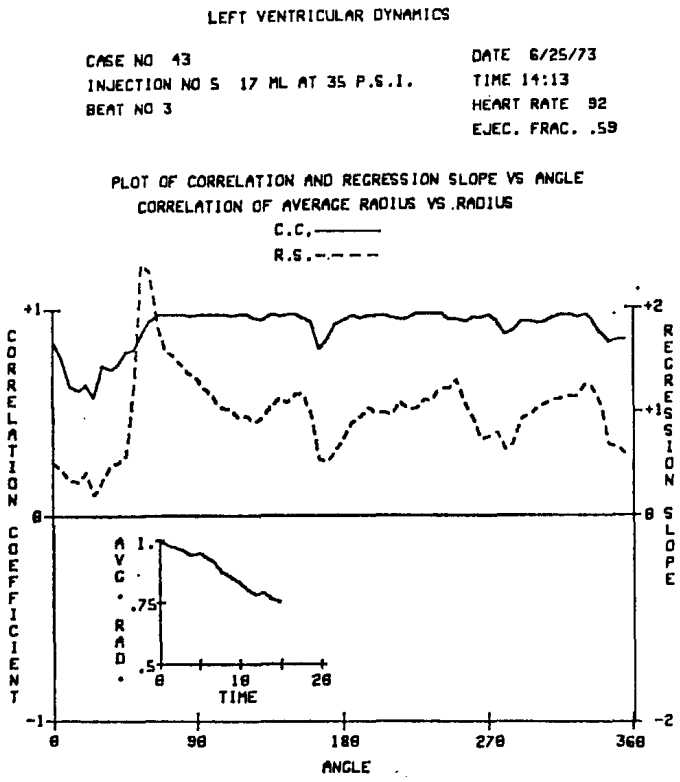

FIG. 3. Plots of correlation coefficients and linear regression slopes for a beat with normal electrical conduction through the ventricle.

through the ventricle. The plots in Fig. 2 show that for this systole the aortic valve motion is poorly correlated with the average motion of the ventricle and that the mitral valve is essentially akinetic. When compared to Fig. 2, the plots in Fig. 3 indicate that, in general, the segments of the ventricular wall contract more in synchrony as the ejection fraction increases. The segment of the endocardial surface showing the greatest change from Fig. 2 to Fig. 3 is the area around and including the mitral valve which had gone from the least active segment to the most active segment as is shown by the large change in the linear regression slopes for this segment. In Fig. 3 the range of values of the regression slope for the angles from 120° to 350° is considerably less than for the corresponding angles in Fig. 2. In addition, the linear regression slopes in Fig. 3 have less variation (standard deviation

of .40 for the data in Fig. 3 versus a standard deviation of .56 for the data in Fig. 2) about the +1 value, again implying that the wall motion is more uniform for the beat with the higher ejection fraction.

The data for Fig. 4 is from a postextrasystolic beat which has an even higher ejection fraction than either of the two normal beats described in Figs. 2 and 3. The plots in Fig. 4 indicate that the heart motion is even more synchronous than

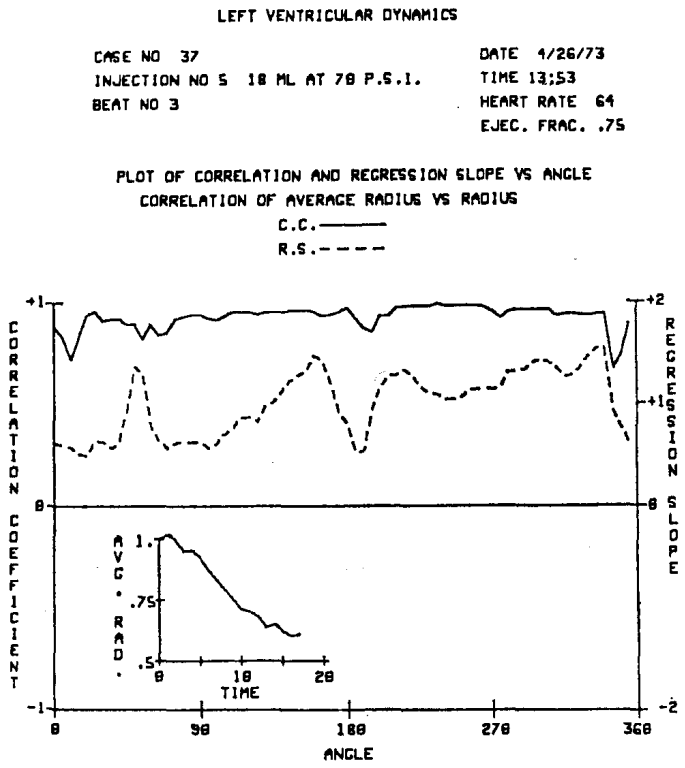

FIG. 4. Plots of correlation coefficients and linear regression slopes for an electrically normal beat following an extrasystolic beat and the related compensatory pause. The ejection fraction is .75 for this beat.

the data shown in Fig. 3 because the correlation coefficient are nearly +1 for all angles and the variation of the linear regression slopes (standard deviation of .32) has decreased even further about the +1 value. The videoangiocardiographic data shows that the ventricle is more distended at end-diastole following the postextrasystolic contraction compared to the end-diastolic area for a normal beat on the same dog, described in Fig. 2, and that all segments of the endocardial wall do, in fact, move more uniformly during systole.

Figure 5 shows the plots of correlation coefficients and linear regression slopes for a pathologically different beat from the contractions just described. The plots represent an example of what happens to the myocardial kinetics when mercury is injected into the anterior descending branch of the left coronary artery, blocking the supply of oxygen and nutrients to a large portion of the left ventricular wall

viewed in the RAO projection used in this study. Two hours following the injection of mercury the left ventriculogram showed that the ventricle was dilated and many segments of the cardiac wall appeared akinetic. Even though the data shown in Fig. 5 is from a postextrasystolic contraction, the ejection fraction was only .39. Figure 5 shows that a large portion of the cardiac wall from 145° to 315° is essentially

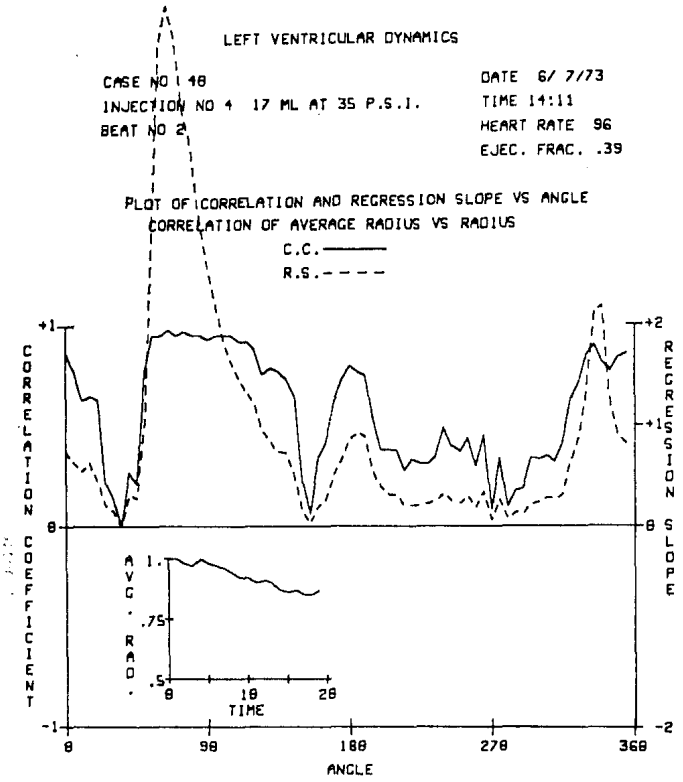

FIG. 5. Plots of correlation coefficients and linear regression slopes for a systole from a heart in which an area of infarction has been created by the injection of approximately .1 ml of mercury into the anterior descending branch of the left coronary artery. The mercury occluded portions of the coronary arteries supplying blood to the lower anterior free wall, apex, and lower posterolateral wall.

akinetic. It also indicates that most of the contraction of the ventricular wall occurs on both sides of the aortic valve, including the mitral valve, as is seen by the high regression slope values at the angles from 55° to 120° and 330° to 360°. Because of the very slight change in the average radius as a function of time, segments of the wall which demonstrate normal motion will be accentuated, as is shown by the high linear regression slopes at 90°. Again, the direct viewing of the angiocardiogram for this contraction confirms the interpretation of the plots in Fig. 5 where specks of mercury can be seen in those portions of the wall which Fig. 5 showed to be akinetic. The location and extent of the injured area was later verified by post mortem examination.

Establishment of the Normal

It was clear when the first plots of correlation coefficients and regression slopes were made for normal beats as in Fig. 2 and postextrasystolic beats as in Fig. 4, that there was a significant difference in the configuration of these plots. The dynamic geometry of the ventricle is obviously different under differing physiological conditions. It also became clear that there is a significant amount of variability in the dynamic geometry of the left ventricle from one normal beat to the next. This is shown by comparing Figs. 2, 3, and 4 and noting that Fig. 3 looks more like Fig. 4 than like Fig. 2. Finally, it appeared as if some of the variation of the correlation

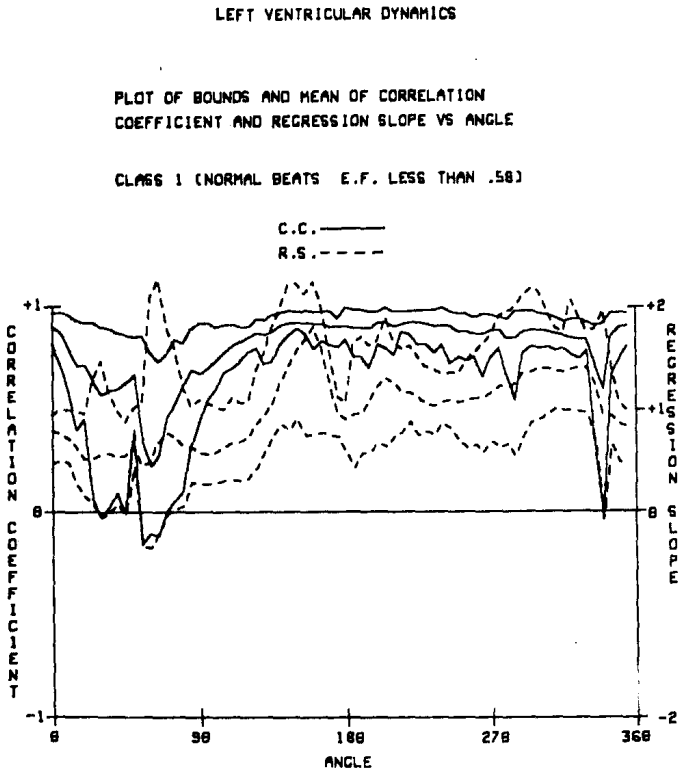

FIG. 6. Plots of the mean, upper, and lower bounds of correlation coefficients (solid lines) and linear regression slopes (dashed lines) for 11 beats with normal electrical conduction and ejection fractions less than .58. These are called class 1 beats.

coefficients and regression slopes were systematic. The data was first separated into groups by heart rate, a separation which proved to have little effect on reducing intragroup variability in the contraction patterns. Next the data was separated by ejection fraction. An arbitrary dividing line using an ejection fraction of .58 was chosen for the normal data, resulting in three data classes which are: (1) normal beats with an ejection fraction less than .58, (2) normal beats with an ejection fraction greater than or equal to .58, and (3) postextrasystolic beats. The ejection fractions for the postextrasystolic beats exceeded those values from all normal beats. The plots of correlation coefficients and linear regression slopes for classes 2 and 3

turned out to be very similar when the data was thus divided. Tables were compiled and plots generated for the maximum, minimum, and mean correlation coefficients and linear regression slopes at each angle for each of the three classes of data. These plots are shown in Figs. 6, 7, and 8, with the mean correlation coefficients and upper and lower bounds shown by the solid lines and the corresponding regression slope values by the dashed lines. As the ejection fraction increases the range of both

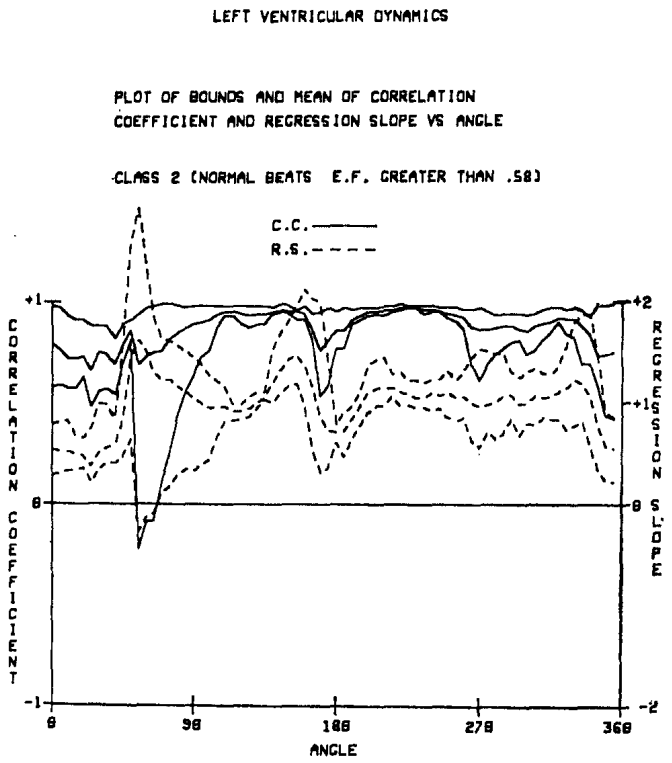

FIG. 7. Plots of mean, upper, and lower bounds of correlation coefficients and linear regression slopes for seven electrically normal beats with ejection fractions greater than or equal to .58.

the correlation coefficient and regression slope decreases, showing that there is not only an increase in uniformity of contraction within the heart but also from beat-to-beat and dog-to-dog as the ejection fraction increases. Separation of the data into these three classes reduces the range of the correlation coefficients and linear regression slopes and thereby facilitates discrimination between normal and abnormal kinetics.

Discrimination of the Abnormals from the Normals

Segments of the cardiac wall which show abnormal kinetics are found automatically by the computer by comparing the values of correlation coefficient and linear regression slope at each angle increment from the suspected abnormal contraction with values for the corresponding normal class to determine which, if

any, values fall outside the normal range. Figure 9 shows the output of such a comparison. The data on the left shows the radius number, angle, and correlation coefficient and regression slope means and ranges for class 3 data (postextrasystolic). On the right are listed the values of the correlation coefficients and regression slopes for the plots in Fig. 5. To the right of each of these latter values is placed a plus (+) or a minus (–) sign to indicate whether that particular value falls

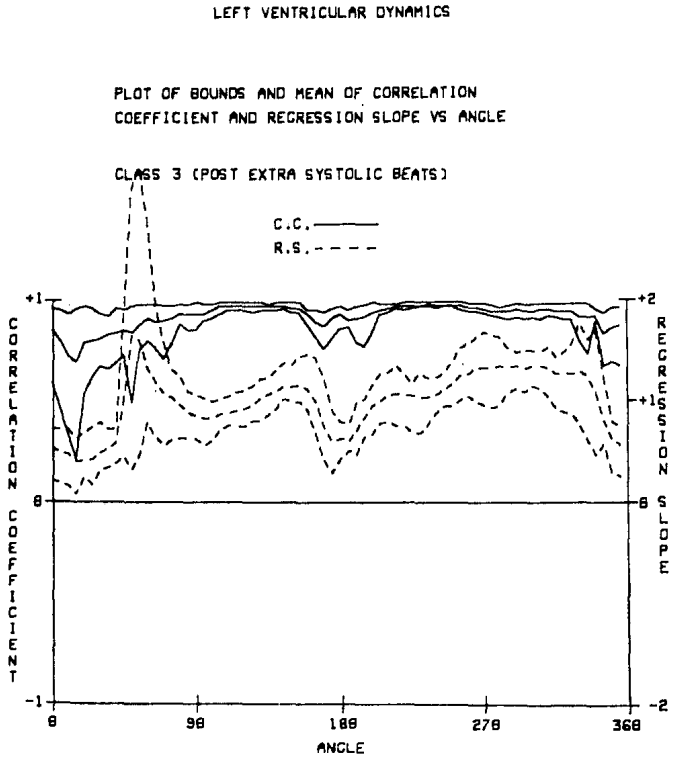

FIG. 8. Plots of the mean, upper, and lower bounds of correlation coefficients and linear regression slopes for seven postextrasystolic beats with normal electrical conduction patterns. These beats are called class 3 data.

above (+) or below (–) the range of normals for this class of data. The same interpretation made from the description of Fig. 5 can be made quantitatively from this table. The angles from 60° to 120° all have regression slope values greater than any of the postextrasystolic beats processed, while the wide segment from 135° to 320° with the exception of the apex have regression slopes and correlation coefficients less than the normal range.

The data in Fig. 9 shows the exact angles of the segments of the left ventricular wall which are under-performing and which segments are compensating. In addition, the table shows how great the deviations from normal are. This demonstrates the primary functions of the mathematical model which are to describe the motion of the ventricular wall during systole, and to locate and quantitate segments of the left ventricular wall which demonstrate abnormal kinetics.

RADIUS	ANGLE	CORR. COEFF. MEAN	CORR. COEFF. RANGE	REG. SLOPE MEAN	REG. SLOPE RANGE	INFARCT CORR	INFARCT REG
1	0	.85	(.59 TO .96)	.53	(.21 TO .73)	.86	.74+
2	5	.80	(.46 TO .95)	.49	(.18 TO .72)	.77	.63
3	10	.72	(.33 TO .93)	.46	(.15 TO .72)	.63	.55
4	15	.69	(.21 TO .96)	.40	(.07 TO .63)	.65	.64+
5	20	.70	(.54 TO .97)	.41	(.24 TO .69)	.63	.46
6	25	.80	(.62 TO .96)	.42	(.17 TO .74)	.22-	.21
7	30	.81	(.67 TO .93)	.49	(.32 TO .79)	.14-	.15-
8	35	.83	(.66 TO .92)	.53	(.34 TO .72)	0-	0-
9	40	.84	(.69 TO .96)	.59	(.39 TO .73)	.27-	.32-
10	45	.85	(.73 TO .95)	1.01	(.45 TO 1.83)	.21-	.27-
11	50	.84	(.49 TO .97)	1.65	(.33 TO 3.12)	.77	1.03
12	55	.88	(.76 TO .98)	1.59	(.47 TO 3.33)	.95	2.86
13	60	.91	(.80 TO .98)	1.33	(.79 TO 2.79)	.95	4.78+
14	65	.89	(.76 TO .98)	1.19	(.64 TO 1.96)	.98	5.86+
15	70	.90	(.71 TO .97)	1.08	(.56 TO 1.59)	.95	4.90+
16	75	.91	(.79 TO .97)	1.02	(.62 TO 1.30)	.97	4.17+
17	80	.93	(.88 TO .98)	.95	(.63 TO 1.25)	.95	3.85+
18	85	.93	(.85 TO .98)	.88	(.62 TO 1.09)	.95	3.09+
19	90	.93	(.85 TO .99)	.85	(.62 TO 1.06)	.93	2.63+
20	95	.93	(.90 TO .98)	.82	(.56 TO 1.02)	.95	2.24+
21	100	.95	(.91 TO .98)	.83	(.61 TO .99)	.95	1.87+
22	105	.97	(.93 TO .99)	.87	(.70 TO 1.02)	.95	1.64+
23	110	.97	(.95 TO .99)	.89	(.76 TO 1.05)	.92-	1.48+
24	115	.97	(.95 TO .99)	.90	(.76 TO 1.09)	.92-	1.39+
25	120	.97	(.95 TO .99)	.93	(.75 TO 1.10)	.88-	1.23+
26	125	.97	(.94 TO .99)	.96	(.81 TO 1.15)	.76-	.96
27	130	.97	(.95 TO .99)	1.03	(.81 TO 1.22)	.79-	.85
28	135	.97	(.95 TO .98)	1.07	(.87 TO 1.23)	.77-	.74-
29	140	.97	(.95 TO .99)	1.10	(.93 TO 1.31)	.73-	.73-
30	145	.97	(.96 TO .99)	1.15	(1.02 TO 1.38)	.65-	.52-
31	150	.96	(.94 TO .99)	1.14	(.99 TO 1.36)	.23-	.15-
32	155	.96	(.94 TO .99)	1.16	(1.00 TO 1.45)	.06-	.03-
33	160	.93	(.88 TO .95)	1.11	(.90 TO 1.47)	.34-	.20-
34	165	.89	(.82 TO .95)	.99	(.67 TO 1.42)	.42-	.28-
35	170	.87	(.76 TO .94)	.75	(.41 TO 1.23)	.62-	.51
36	175	.91	(.81 TO .96)	.60	(.29 TO .90)	.73-	.66
37	180	.93	(.86 TO .97)	.63	(.43 TO .79)	.80-	.87+
38	185	.90	(.87 TO .95)	.60	(.51 TO .77)	.77-	.94+
39	190	.91	(.79 TO .97)	.70	(.47 TO .99)	.75-	.89
40	195	.92	(.77 TO .98)	.84	(.65 TO 1.02)	.53-	.55-
41	200	.94	(.84 TO .99)	.96	(.67 TO 1.16)	.38-	.38-
42	205	.95	(.93 TO .98)	1.01	(.78 TO 1.27)	.38-	.31-
43	210	.96	(.94 TO .98)	1.06	(.80 TO 1.29)	.38-	.31-
44	215	.97	(.96 TO .98)	1.07	(.75 TO 1.35)	.28-	.21-
45	220	.97	(.95 TO .99)	1.06	(.75 TO 1.27)	.33-	.21-
46	225	.97	(.96 TO .99)	1.05	(.69 TO 1.18)	.31-	.22-
47	230	.97	(.97 TO .99)	1.03	(.68 TO 1.27)	.31-	.23-
48	235	.98	(.97 TO .99)	1.04	(.76 TO 1.22)	.35-	.26-
49	240	.97	(.96 TO .99)	1.06	(.88 TO 1.23)	.49-	.33-
50	245	.97	(.97 TO .99)	1.11	(.95 TO 1.28)	.40-	.25-
51	250	.97	(.97 TO .99)	1.17	(.95 TO 1.37)	.37-	.23-
52	255	.97	(.95 TO .99)	1.25	(1.01 TO 1.52)	.44-	.30-
53	260	.96	(.94 TO .98)	1.27	(1.05 TO 1.57)	.30-	.19-
54	265	.96	(.94 TO .98)	1.32	(.99 TO 1.62)	.45-	.34-
55	270	.95	(.93 TO .98)	1.33	(.95 TO 1.68)	.08-	.06-
56	275	.94	(.92 TO .97)	1.33	(.93 TO 1.64)	.34-	.27-
57	280	.94	(.91 TO .96)	1.34	(.96 TO 1.63)	.10-	.08-
58	285	.94	(.90 TO .97)	1.33	(1.08 TO 1.52)	.18-	.14-
59	290	.95	(.91 TO .98)	1.34	(1.12 TO 1.47)	.19-	.13-
60	295	.94	(.90 TO .97)	1.32	(1.08 TO 1.50)	.34-	.22-
61	300	.94	(.91 TO .98)	1.34	(1.14 TO 1.49)	.33-	.25-
62	305	.95	(.90 TO .98)	1.34	(1.11 TO 1.49)	.35-	.29-
63	310	.95	(.92 TO .98)	1.32	(1.03 TO 1.53)	.32-	.27-
64	315	.94	(.91 TO .98)	1.26	(.92 TO 1.43)	.41-	.32-
65	320	.94	(.90 TO .98)	1.27	(.88 TO 1.49)	.63-	.62-
66	325	.94	(.90 TO .98)	1.26	(.86 TO 1.57)	.71-	.88
67	330	.91	(.78 TO .98)	1.29	(.75 TO 1.76)	.85	1.37
68	335	.91	(.73 TO .98)	1.23	(.61 TO 1.60)	.90	2.13+
69	340	.92	(.89 TO .95)	1.07	(.46 TO 1.69)	.81-	2.19+
70	345	.83	(.67 TO .93)	.78	(.57 TO 1.24)	.77	1.21
71	350	.86	(.69 TO .96)	.62	(.28 TO .78)	.84	.89+
72	355	.87	(.67 TO .96)	.56	(.25 TO .74)	.86	.81+

FIG. 9. Shows the values of radius number, angle, mean and range of the correlation coefficients, and the mean and range of the linear regression slopes for class 3 data (postextrasystolic) compared with the correlation coefficients and linear regression slopes from the abnormal heart described in Fig. 5. To the right of each correlation coefficient and regression slope for the abnormal heart there appears a plus sign (+) if that value is above the normal range for class 3 data and a minus sign (−) if it is below the range. This describes the simple method for locating segmental wall motion disorders.

Discussion

The modeling process described above takes advantage of the merits of the angiocardiographic techniques and has, in a large portion, overcome the disadvantages by reducing and concentrating the large amount of data in an angiogram into two plots of correlation coefficients and linear regression slopes, and presenting quantitative data about dynamic geometry of each segment of the left ventricular wall viewed in a single plane. The two major disadvantages of angiocardiographic methods not solved in this study are the problems of invading the circulation and changing the hemodynamics by injecting a toxic contrast media. These problems have been minimized in two ways. The first way is to process the beats which occur soon after the injection. The second minimizing effect stems from the model itself and how it is used. This model sets up classes of data, determines the ranges of the correlation coefficients and linear regression slopes for differing physiological states, and then determines if the same parameters for a suspected abnormal ventricle fall outside of the normal range. This minimizes the effects of the contrast media because both the normal and abnormal data have these effects superimposed upon them. In addition, the primary use of the model in this study is to separate abnormals from normals and not to describe the normal contraction. This brings up the important point that the model itself is not restricted to use with contour data from videoangiocardiographic procedures. Contour data from two-dimensional images of the heart derived from another signal, such as ultrasonic scanning of the heart, could be modeled in precisely the same manner to yield information about left-ventricular dynamic geometry without the physiological disturbance and risk which accompany contrast media injection.

The data gathering and analysis methods described are designed for both clinical and research applications. The most immediate clinical application is the location of segments of the human myocardium which demonstrate motion abnormalities during systole. While it is true that the cardiologist can detect obvious paradoxical motion from angiocardiograms, as in the case of some aneurysms or large portions of the ventricular wall which are akinetic, he must do the evaluation subjectively. In addition, if the motion abnormality involves a small portion of the ventricular wall or is in the form of a slightly hypokinetic segment, it may not be noticed by simply viewing the ventriculogram. Also the need for making more than one classification of normal data demonstrates that there is a significant variability in normal cardiac kinetics. Further investigation is needed to better determine the nature of the systematic changes of the correlation coefficients and linear regression slopes with changing physiological states and thereby obtain a more accurate method for detecting motion abnormalities. This may provide new insight into the basic physiology of ventricular contraction.

The model could also be used to classify myocardial kinetics in the selection and evaluation of candidates for coronary bypass procedures which have become so

popular. At the present time the surgeon has the ECG, ventriculogram, left ventricular pressure recordings, and the selective coronary arteriogram at his disposal. With these tools he must decide if there are portions of the ventricle which are ischemic and which also might perform better following revascularization. Unfortunately, he cannot often discriminate between scarred (unrecoverable) and ischemic but recoverable portions of the myocardium. This model may provide useful insight to this question. In addition, such a model of ventricular contraction may provide an objective measure of the change in ventricular performance resulting from an operative procedure such as coronary artery vein bypass grafting and lead to better criteria for the selection of patients who would benefit from operation. Much experience with this kind of data in patients who are carefully followed over an extended period will be needed to develop prognostic criteria based on this new tool.

For the researcher, the model provides a tool for studying the effects of different physiological states on the dynamic geometry of the ventricle not only during systole, but also during diastole. The relationship of the sequence of contraction to physiological and pharmacological manipulations may be studied with this technique as never before possible using markers and implanted gauges which at best can provide information about only a limited set of points on the ventricular surface. Such studies will become even more valuable when ventricular border information can be obtained using methods which do not impose abnormal stress on the system being studied. Ultrasound shows promise of providing such a data source.

REFERENCES

1. HAWTHORNE, E. W. Dynamic geometry of the left ventricle: Introduction. *Fed. Proc.* **28,** 1323 (1969).
2. GORLIN, R., KLEIN, M. D., AND SULLIVAN, J. M. Prospective correlative study of ventricular aneurysm. *Am. J. Med.* **42,** 512 (1967).
3. HERMAN, M. V., HEINLE, R. A., KLEIN, M. D., AND GORLIN, R. Localized disorders in myocardial contraction: Asynergy and its role in congestive heart failure. *New Eng. J. Med.* **277,** 222 (1967).
4. RUSHMER, R. E., CRYSTAL, D. K., AND WAGNER, C. The functional anatomy of ventricular contraction. *Circ. Res.* **1,** 162 (1953).
5. HARRISON, D. C., GOLDBLATT, A., AND BRAUWALD, E. Studies on cardiac dimensions in intact, unanesthetized man: Description of techniques and their validation. *Circ. Res.* **13,** 448 (1963).
6. MITCHELL, J. H., AND MULLINS, C. B. "Factors Influencing Myocardial Contractility" (R. D. Tanz, F. Kavaler, and J. Roberts, Eds.), p. 177. Academic Press, New York, 1967.
7. MITCHELL, J. H., WILDENTHAL, K., AND MULLINS, C. B. Geometrical studies of the left ventricle utilizing biplane cinefluorography. *Fed. Proc.* **28,** 1334 (1969).
8. HINDS, J. E., HAWTHORNE, E. W., MULLINS, C. B., AND MITCHELL, J. H. Instantaneous changes in the left ventricular lengths occurring in dogs during the cardiac cycle. *Fed. Proc.* **28,** 1351 (1969).
9. RUSHMER, R. E., CRYSTAL, D. K., WAGNER, C., ELLIS, R. M., AND NASH, A. A. Continuous measurements of left ventricular dimensions in intact, unanesthetized dogs. *Circ. Res.* **2,** 14 (1954).

10. RUSHMER, R. E. Pressure-circumference relations of left ventricle. *Am. J. Physiol.* **186,** 115 (1956).
11. HAWTHORNE, E. W. Instantaneous dimensional changes of the left ventricle in dogs. *Circ. Res.* **9,** 110 (1961).
12. FEIGL, E. O., AND FRY, D. L. Myocardial mural thickness during the cardiac cycle. *Circ. Res.* **14,** 541 (1964).
13. NINOMIYA, I., AND WILSON, M. F. Analysis of ventricular dimensions in the unanesthetized dog. *Circ. Res.* **16,** 249 (1965).
14. HAWTHORNE, E. W. Dynamic geometry of the left ventricle. *Am. J. Cardiol.* **18,** 566 (1966).
15. KRAUNZ, R. F., AND KENNEDY, J. W. Ultrasonic determination of left ventricular wall motion in man: Studies at rest and after exercise. *Am. Heart J.* **79,** 36 (1970).
16. KAZAMIAS, T. M., GANDER, M. P., ROSS, J., JR., AND BRAUNWALD, E. Detection of left-ventricular wall motion disorders in coronary artery disease by radarkymography. *New Eng. J. Med.* **285,** 3 (1971).
17. ROBB, G. P., AND STEINBERG, I. I. A practical method of visualization of the chambers of the heart, the pulmonary circulation, and the great blood vessels in man. *J. Clin. Inves.* **17,** 507 (1938).
18. RUSHMER, R. E., AND CRYSTAL, D. K. Changes in the configuration of the ventricular chambers during the cardiac cycle. *Circulation* **4,** 211 (1951).
19. CHATTERJEE, K., SWAN, H. J. C., PARMLEY, W. W., SUSTAITA, H., MARCUS, H. S., AND MATLOFF, J. Influence of direct myocardial revascularization on left ventricular asynergy and function in patients with coronary heart disease. *Circulation* **47,** 276 (1973).
20. TSAKIRIS, A. G., DONALD, D. E., STURM, R. E., AND WOOD, E. H. Volume, ejection fraction, and internal dimensions, of left ventricle by biplane videometry. *Fed. Proc.* **28,** 1358 (1969).
21. LANE, F. J., CARROL, J. M., LEVINE, H. D., AND GORLIN, R. The apexcardiogram in myocardial asynergy. *Circulation* **37,** 890 (1968).
22. LLUCH, S., MOUGUILEVSKY, H. G., PIETRA, G., SHAFFER, A. B., HIRSCH, L. J., AND FISHMAN, A. P. A reproducible model of cardiogenic shock in dog. *Circulation* **39,** 205 (1969).
23. CLAYTON, P. D., HARRIS, L. D., RUMEL, S. R., AND WARNER, H. R. Left ventricular videometry. *Comp. Biomed. Res.* **7,** 369 (1974).